Resistive upper critical fields and irreversibility lines of optimally doped high-T_c cuprates

Yoichi Ando

Bell Laboratories, Lucent Technologies, 700 Mountain Avenue, Murray Hill, New Jersey 07974
and Central Research Institute of Electric Power Industry, Komae, Tokyo 201-8511, Japan

G. S. Boebinger, A. Passner, and L. F. Schneemeyer

Bell Laboratories, Lucent Technologies, 700 Mountain Avenue, Murray Hill, New Jersey 07974

T. Kimura, M. Okuya, S. Watauchi, J. Shimoyama, and K. Kishio

Department of Applied Chemistry, University of Tokyo, Hongo, Bunkyo-ku, Tokyo 113, Japan

K. Tamasaku, N. Ichikawa, and S. Uchida

Superconductivity Research Course, University of Tokyo, Yayoi, Bunkyo-ku, Tokyo 113, Japan

We present the resistively determined upper critical field $H^\rho_{c2}(T)$ and the irreversibility lines $H^\rho_{\mathrm{irr}}(T)$ of various high-T_c cuprates, deduced from measurements in 61-T pulsed magnetic fields applied parallel to the c axis. The *shape* of both $H^\rho_{c2}(T)$ and $H^\rho_{\mathrm{irr}}(T)$ depends monotonically on the anisotropy of the material and none of the samples show saturation of $H^\rho(T)$ at low temperatures. The anomalous positive curvature $d^2 H^\rho/dT^2 > 0$ is the strongest in materials with the largest normal state anisotropy, regardless of whether anisotropy is varied by changing the carrier concentration or by comparing a variety of optimally doped compounds. [S0163-1829(99)10341-2]

The anisotropy of the high-T_c cuprates, coupled with their short coherence lengths, gives rise to a complex magnetic phase diagram, featuring a vortex liquid state located between the vortex solid and the normal state.[1–3] In particular, in the high-T_c cuprates, the vortex lattice can melt at temperatures well below the onset of short-range superconducting order occurring at the upper critical magnetic field H_{c2}. In a fixed temperature experiment, this is evidenced by the onset of resistivity due to vortex motion well below the magnetic field at which the normal-state resistivity is restored, defined as the resistively determined upper critical magnetic field $H^\rho_{c2}(T)$. Resistivity measurements on overdoped $Tl_2Ba_2CuO_y$ (Tl-2201) (Ref. 4) and overdoped $Bi_2Sr_2CuO_y$ (Bi-2201) (Ref. 5) have found a strong upward curvature in $H^\rho_{c2}(T)$ with no evidence of saturation at low temperatures. Such an $H^\rho_{c2}(T)$ curve contrasts strongly with the conventional Werthamer-Helfand-Hohenberg (WHH) theory for superconductors with weak electron-phonon coupling,[6] in which $H_{c2}(T)$ exhibits negative curvature and saturates at low temperatures. Similarly anomalous $H^\rho_{c2}(T)$ curves have been discussed in connection with other anisotropic superconductors, such as the organic superconductors.[7] However, due to the extremely large upper critical fields, studies of the resistive transition in the cuprates have been largely limited to samples in which T_c and H_{c2} are greatly suppressed,[8] either in strongly underdoped[9] or overdoped samples,[4,5] in deliberately impurity-doped samples,[10] or in the electron-doped cuprates.[11]

In addition to the unusual "shape" of the $H^\rho_{c2}(T)$ curves, a reexamination of the origin and meaning of the resistive transition in the cuprates is fueled, in part, by specific heat,[12] Raman spectroscopy,[13] and magnetization[14] measurements which indicate that the onset of local superconducting order [generally interpreted as the mean-field $H_{c2}(T)$] in Tl-2201 occurs at magnetic fields well above $H^\rho_{c2}(T)$. At this mean-field $H_{c2}(T)$, no feature is observed in the measured resistivity. Perhaps more surprisingly, the experimental evidence for this mean-field $H_{c2}(T)$, in both the specific heat and Raman experiments, is anomalously and dramatically suppressed by magnetic fields of only a few T. Thus, $H^\rho_{c2}(T)$ does not seem to correspond to the mean-field $H_{c2}(T)$, which might suggest that it corresponds to the melting of the vortex lattice. The difficulty with this interpretation of $H^\rho_{c2}(T)$ is that it is unclear why the melted vortex state should be (or can be) indistinguishable in resistivity measurements from the normal state. More specifically, if $H^\rho_{c2}(T)$ corresponds to the irreversibility line, then the magnetic phase diagram (at least for Tl-2201 and Bi-2201) contains an unusual vortex liquid state whose resistivity apparently equals the normal-state resistivity and exhibits no substantial magnetic-field or temperature dependence.[4,5] In light of the debate about the magnetic phase diagram and the interpretation of $H^\rho_{c2}(T)$ in the cuprates, a systematic study of $H^\rho_{c2}(T)$, particularly in optimally doped compounds, is clearly desirable.

In this paper, we present resistivity measurements in 61-T pulsed magnetic fields which determine $H^\rho_{c2}(T)$ for $La_{2-x}Sr_xCuO_4$ (LSCO) of various carrier concentrations x. In addition to LSCO, we present $H^\rho_{c2}(T)$ data for nearly optimally doped $Bi_2Sr_2CaCu_2O_y$ (Bi-2212) and $YBa_2Cu_3O_{7-\delta}$ (YBCO). We find that the "shape" of the $H^\rho_{c2}(T)$ changes monotonically with the anisotropy of the normal state of the sample, becoming more conventional as the anisotropy gets smaller. The magnitude of the positive curvature in $H^\rho_{c2}(T)$, along with the steep slope of $H^\rho_{c2}(T)$ at the lowest experimental temperature, are the greatest in the most anisotropic compounds.
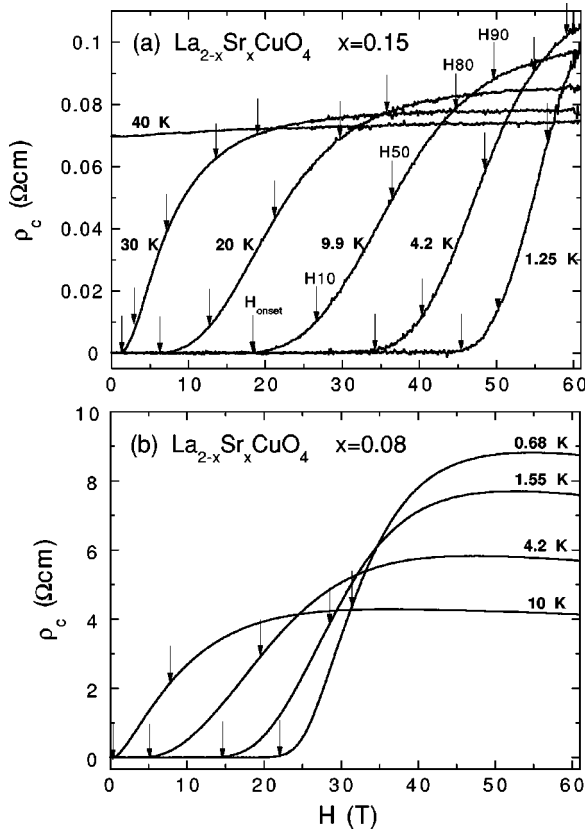
　　　　　PRB <u>60</u>　　　12 475

FIG. 1. Selected traces of ρ_c vs H of (a) optimally doped LSCO ($x=0.15$) and (b) underdoped LSCO ($x=0.08$) at fixed temperatures. The arrows in (a), explicitly labeled for the $T=9.9$ K trace, mark the onset, 10, 50, 80, and 90 % points of each resistive transition. Only H_{onset} and $H50$ are marked by arrows in (b).

The LSCO crystals, grown by the traveling-solvent floating-zone method by the University of Tokyo groups, have been previously studied in pulsed magnetic fields;[15] the samples reported here with Sr concentrations $x=0.08$ and 0.17 are grown by the Kishio group and those with $x=0.15$ are grown by the Uchida group. The Bi-2212 crystals, grown by the Kishio group using the floating-zone method, are heat treated in sealed quartz tubes to tune to the near-optimum doping. Finally, the YBCO crystals are grown at Bell Laboratories by a flux method in zirconia crucibles and annealed in sealed quartz tubes to tune the oxygen content to optimal doping. The resistivity of each sample was measured at a given fixed temperature during the magnetic field pulse using a ~ 100 kHz lockin technique.[15,16] No significant eddy current heating resulted from the time-varying magnetic field. To avoid additional dissipation due to vortex depinning in response to an applied Lorenz force, the current was applied parallel to the magnetic field (along the c axis), except in the case of the YBCO crystal, whose shape and the relatively small electrical anisotropy precluded this geometry.

Figure 1(a) shows a representative set of raw experimental traces, the c-axis resistivity ρ_c vs H of LSCO ($x=0.15$) at various temperatures. The onset field H_{onset} is defined as the magnetic field at which the resistivity first is detected to deviate from zero in the ρ vs H plot. This definition is our best determination of the irreversibility line, given the limited sensitivity of the pulsed-field data. To characterize the

rest of the resistive transition in the H vs T plane, we determine those magnetic fields at which the resistivity equals 10, 50, 80, and 90 % of the ''normal-state'' resistivity, denoted $H10$, $H50$, $H80$, and $H90$, respectively [arrows in Fig. 1(a)]. In traditional superconductors, $H50$ is often associated with the mean-field upper critical field H_{c2}; however, given the uncertain interpretation of the resistive transition in the cuprates, we make no *a priori* determination of $H_{c2}^{\rho}(T)$ from the data. [We do note, in passing, that $H80(T)$ is comparable to one common assignment of $H_{c2}^{\rho}(T)$: the intersection of two straight line extrapolations from the normal state resistivity and the steepest slope in the transition region.]

At the lowest temperatures, as Fig. 1(a) illustrates, even 61 T can be insufficient to recover the normal state. In this regime, H_{onset} remains unambiguous, but the uncertainties in determining $H10$, $H50$, $H80$, and $H90$ necessarily increase. In this regime, we extrapolate the normal state resistivity to those lower temperatures at which it cannot be measured directly. For the data of Fig. 1(a), this is relatively straightforward since the low-temperature normal-state resistivity in underdoped LSCO obeys a $\log(1/T)$ divergence;[17] for example, we estimate the normal-state resistivity at 1.25 K to be 0.135 Ω cm. The resulting errors in $H10$, etc., are estimated to be about a few T even at the lowest temperatures. For LSCO ($x=0.08$), as shown in Fig. 1(b), no extrapolation is required and thus the errors in $H10$, etc., are rather small, less than 2 T.

Figure 2(a) shows the contours of the resistive transition of LSCO ($x=0.15$) in the H vs T plane, as determined from the data of Fig. 1(a). Representative error bars are attached to the data. Note that the midpoint of the transition, $H50$, shows a conventional linear temperature dependence from T_c down to $T\simeq 0.5T_c$; however, it exhibits a steep rise at low temperatures below ~ 10 K, $T\simeq 0.25$ T_c. Note also that all of the curves exhibit this sharp rise, which persists to the lowest experimental temperature ($T=1.25$ K$\simeq 0.03$ T_c). Thus, regardless of the precise determination of $H_{c2}^{\rho}(T)$ from the ρ_c vs H curves in Fig. 1(a), H_{c2}^{ρ} in optimally doped LSCO exhibits no evidence of saturation at low temperatures, a particularly unusual feature in common with previously-reported data from overdoped Tl-2201 (Ref. 4) and overdoped Bi-2201.[5]

Figure 2(b) shows the contours of the resistive transition for underdoped LSCO ($x=0.08$) in the H vs T plane, constructed from the data of Fig. 1(b). Compared to LSCO ($x=0.15$), the curves in Fig. 2(b) show even greater upward curvature, extending from T_c down to the lowest experimental temperatures for all curves, including $H80(T)$ and $H90(T)$. These data, when coupled with the data for LSCO ($x=0.17$) (shown later), suggest a monotonic dependence in which the magnitude of the upward curvature increases with decreasing carrier concentration. We emphasize that 61 T is sufficient to suppress superconductivity in LSCO ($x=0.08$) and thus all the data points in Fig. 2(b) have rather small error bars. Therefore, even though the raw resistive transition in Fig. 1(b) is much broader compared to the overdoped Tl-2201 (Ref. 4) or Bi-2201 (Ref. 5), all the definitions for H_{c2}^{ρ} are unambiguously indicating an unusual upward curvature of $H_{c2}^{\rho}(T)$ in this underdoped LSCO.
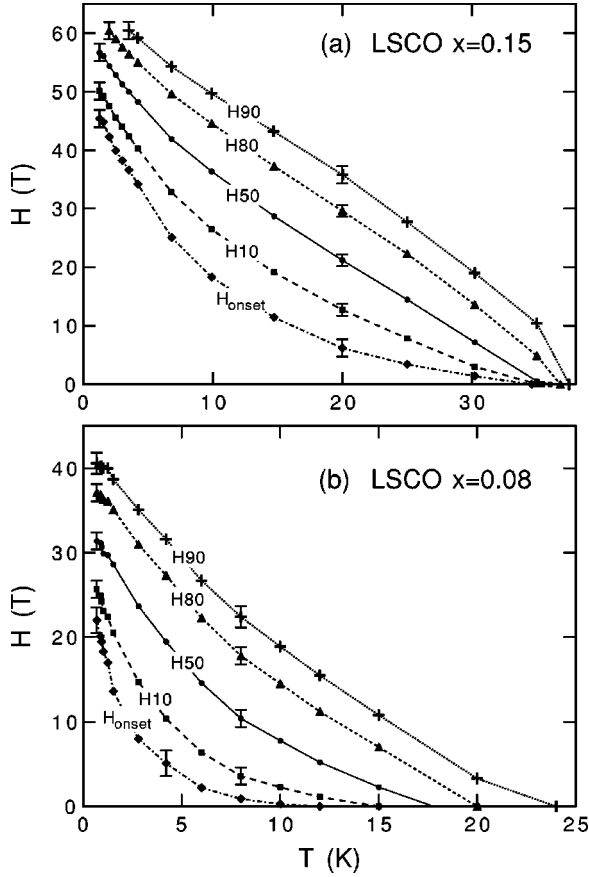
FIG. 2. The resistive transitions for (a) optimally doped LSCO ($x=0.15$) and (b) underdoped LSCO ($x=0.08$) in the H vs T plane, characterized by H_{onset}, $H10$, $H50$, $H80$, and $H90$. Representative error bars are attached to the data.

Figure 3 contains the raw R vs H data for three cuprates near optimum doping, Bi-2212, LSCO ($x=0.17$) and YBCO. One may notice that the data for Bi-2212 [Fig. 3(a)] show some linear background before the resistance rapidly increases; we have not identified the cause of this linear background, but we determined H_{onset} for this sample with the deviation from the linear background. One may also notice that the Bi-2212 data show pronounced negative magnetoresistance in the high-field normal state, particularly at low temperatures.

In Fig. 3, we show the data in resistance, rather than in resistivity, to demonstrate that the noise level of our pulsed-field experiments is not determined by the absolute voltage but changes with the sample impedance; the noise is always about a few percent of the impedance being measured (as long as the impedance is larger than a few tens of mΩ). This fact precludes the usage of the usual criteria for the irreversibility field defined by a certain electric-field threshold. This is the reason why we needed to determine the onset field H_{onset} rather naively with the magnetic field at which the resistivity first is detected to deviate from zero in the ρ vs H plot.

In determining the normal-state resistance R_n for the samples shown in Fig. 3, we used a linear extrapolation from higher temperatures; for example, we estimated R_n to be 33 Ω at 3.0 K for Bi-2212, 1.08 Ω at 1.55 K for LSCO (x
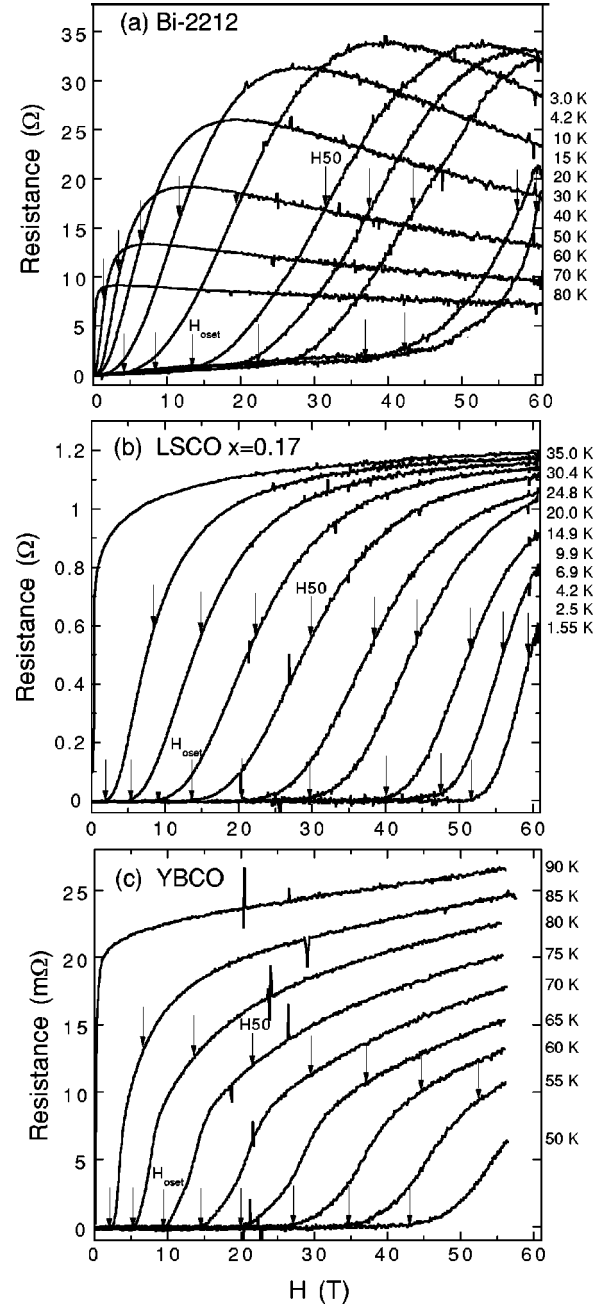

FIG. 3. Selected traces of raw R vs H data for three cuprates near optimal doping, (a) Bi-2212, (b) LSCO ($x=0.17$), and (c) YBCO. The temperatures for the traces are listed on the right. H_{onset} and $H50$ are marked by arrows on the traces.

$=0.17$), and 14.6 mΩ at 50 K for YBCO. One can infer from Fig. 3 that R_n of Bi-2212 and LSCO ($x=0.17$) becomes relatively temperature independent at low temperatures and therefore the errors involved in the estimation of R_n are relatively small compared to that for YBCO. The data in Fig. 3(c) show large positive ''magnetoresistance,'' particularly at lower temperatures, which makes the definition of R_n rather ambiguous. As a result, the estimated errors for $H10$, etc., are comparatively large for YBCO. These very broad resistive transitions of YBCO suggest that the idea of the ''resistive upper critical field'' at which the normal-state resistivity is restored might be a questionable concept for some of the high-T_c cuprates.
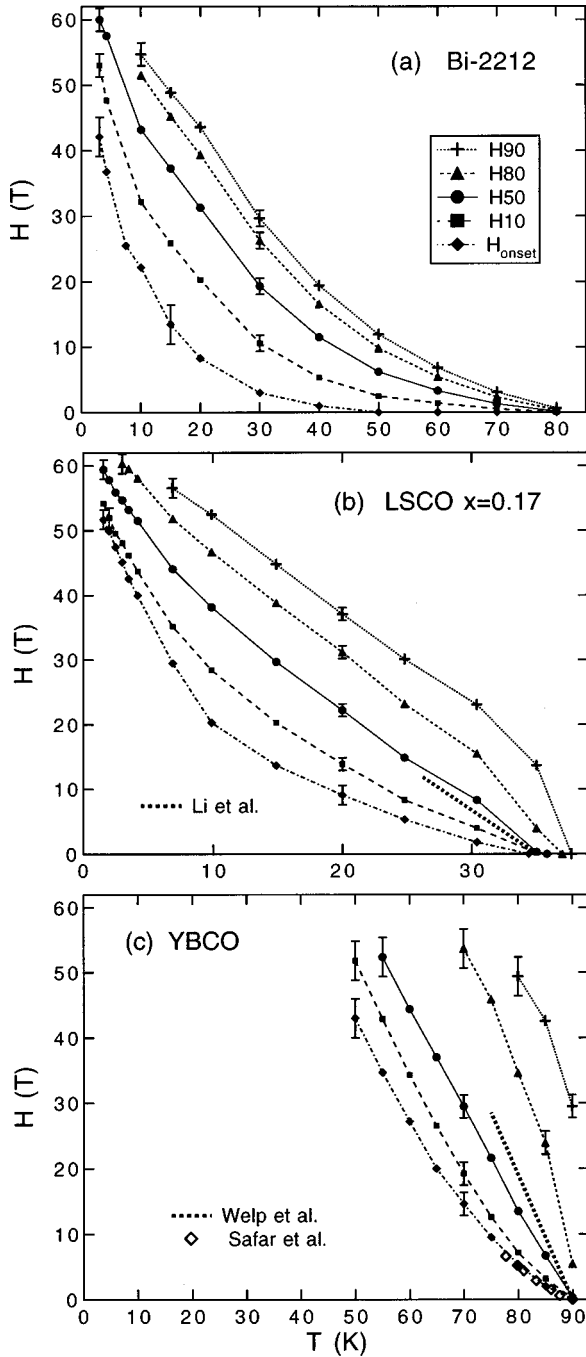
FIG. 4. The contours of the resistive transition in the H vs T plane for three cuprates at near optimum doping: (a) Bi-2212, (b) LSCO ($x=0.17$), and (c) YBCO. The thick dashed lines in (b) and (c) are magnetically determined H_{c2} lines (Refs. 18, 19). The open diamonds in (c) give the vortex lattice melting line obtained by Safar *et al.* (Ref. 20). Note that the panels are arranged in order of decreasing normal-state anisotropy, ρ_c/ρ_{ab}. Representative error bars are attached to the data.

Figure 4 shows the contours of the resistive transitions in the H vs T plane for the three cuprates at near optimum doping, deduced from the data in Fig. 3. Representative error bars are attached to the data. To corroborate the pulsed-magnetic-field data with more conventional measurements, we also plot the $H_{c2}(T)$ lines determined from the reversible magnetization (thick dashed lines): in Fig. 4(b), for LSCO

($x=0.17$) crystals from the same source[18] and, in Fig. 4(c), the frequently cited line of -1.9 T/K for YBCO.[19] Note that in each case the H_{c2} line determined from the reversible magnetization lies near the midpoint of the resistive transition, the $H50$ line. In Fig. 4(c), the open diamonds denote the first-order vortex lattice melting transition line obtained by Safar *et al.*[20] and this line agrees quite well with our H_{onset} (filled diamonds).

The data in Fig. 4 are arranged in order of decreasing normal-state anisotropy, ρ_c/ρ_{ab}. Note that the anomalous upward curvature $d^2H^\rho/dT^2>0$ is greatest in the more anisotropic materials. This curvature decreases monotonically, until for YBCO the $H80$ and $H90$ curves exhibit the more conventional negative curvature. We note that this trend does not depend monotonically on the magnitude of T_c, for example. Furthermore, observation of this trend among different optimally doped cuprates suggests that the carrier-concentration dependence found in LSCO may arise simply from the decreasing normal-state anisotropy which accompanies increasing carrier concentration.

The H vs T diagrams shown in Figs. 2 and 4 clearly indicate that, for all the cuprates studied, the unconventional upward curvature is common for H_{onset} over the entire temperature range studied here. The anisotropy and short coherence length of the cuprates give a phase diagram with a vortex liquid regime between the vortex solid and the normal state.[3] The width of the vortex liquid regime is expected to increase with increasing anisotropy.[21] It is most likely that our H_{onset} is closely related to the irreversibility line $H_{\mathrm{irr}}(T)$ associated with the vortex liquid-to-solid transition, which would be expected to exhibit the observed monotonic dependence on anisotropy.

The interpretation of the rest of the resistive transition, characterized by the $H10$, $H50$, $H80$, and $H90$ curves of Figs. 2 and 4, is not so clear. Nonetheless, obvious trends appear in the data. For all the cuprates studied, the unconventional upward curvature seen in H_{onset} is also seen in $H10$ and $H50$ over the entire temperature range studied; however, the upward curvature is observed in the higher resistance contours, $H80$ and $H90$, only in such highly anisotropic systems as Bi-2212 or underdoped LSCO. On the other hand, the lack of saturation of $H_{c2}^\rho(T)$ at low temperatures seems to be a more robust feature of the resistive transition. Thus, while there is a substantial literature addressing the resistive transition and $H_{c2}^\rho(T)$ in the cuprates,[7] a successful theory would need to account for the following new phenomenology: (i) Among the optimally doped cuprates, $H_{c2}^\rho(T)$ can exhibit a global positive curvature, but only in the more anisotropic compounds. (ii) As the anisotropy is decreased, the anomalous upward curvature disappears near T_c in the upper part of the resistive transition, i.e., in the $H80$ and $H90$ curves. (iii) There is no evidence of saturation in $H_{c2}^\rho(T)$ in any of the cuprates studied in the low temperature limit.

Several dramatically contrasting models for $H_{c2}(T)$ have found global positive curvature: for example, localization of charged bosons in the small coherence length limit,[22] scattering from magnetic impurities which order at low temperatures,[23] influence of a quantum critical point associated with melting of the vortex lattice,[24] and mixing of d_{xy} and $d_{x^2-y^2}$ components due to the magnetic field.[25] For many of the above models, the effect of anisotropy is not yet

clear. Our data clearly indicate that the normal state anisotropy plays a key role, perhaps *the* key role, in determining the curvature of $H_{c2}^{\rho}(T)$.

In summary, we characterize the resistive transition for a variety of optimally doped high-T_c cuprates using 61-T pulsed magnetic fields. The anomalous positive curvature of both $H_{c2}^{\rho}(T)$ and $H_{irr}^{\rho}(T)$ is strongest in the more anisotropic cuprates. None of the samples studied show saturation of $H_{c2}^{\rho}(T)$ or $H_{irr}^{\rho}(T)$ at low temperatures.

[1] D.S. Fisher, M.P.A. Fisher, and D.A. Huse, Phys. Rev. B **43**, 130 (1991).

[2] H. Safar, P.L. Gammel, D.A. Huse, D.J. Bishop, W.C. Lee, J. Giapintzakis, and D.M. Ginsberg, Phys. Rev. Lett. **70**, 3800 (1993).

[3] For review, see D.E. Farrell, in *Physical Properties of High Temperature Superconductors IV*, edited by D.M. Ginsberg (World Scientific, Singapore, 1994).

[4] A.P. Mackenzie, S.R. Julian, G.G. Lonzarich, A. Carrington, S.D. Hughes, R.S. Liu, and D.C. Sinclair, Phys. Rev. Lett. **71**, 1238 (1993).

[5] M.S. Osofsky, R.J. Soulen, Jr., S.A. Wolf, J.M. Broto, H. Rakoto, J.C. Ousset, G. Coffe, S. Askenazy, P. Pari, I. Bozovic, J.N. Eckstein, and G.F. Virshup, Phys. Rev. Lett. **71**, 2315 (1993).

[6] N.R. Werthamer, E. Helfand, and P.C. Hohenberg, Phys. Rev. **147**, 295 (1966).

[7] For a review, see B. Brandow, Phys. Rep. **296**, 1 (1998).

[8] An exception is an experiment using explosively generated microsecond magnetic fields [X. Smith *et al.*, J. Supercond. **7**, 269 (1994)], suggesting that $H_{c2}^{\rho}(T)$ of optimally doped YBCO is consistent with WHH theory; however, $H_{c2}^{\rho}(T)$ in these difficult measurements is defined at a given fixed $T<T_c$, not by any observed feature in the $\rho(B)$ data, but rather by the magnetic field at which the measured $\rho(B)$ equals the normal state resistivity at $T=T_c$.

[9] K. Karpinska, A. Malinowski, Marta Z. Cieplak, S. Guha, S. Gershman, G. Kotliar, T. Skoskiewicz, W. Plesiewicz, M. Berkowski, and P. Lindenfeld, Phys. Rev. Lett. **77**, 3033 (1997).

[10] D.J.C. Walker, O. Laborde, A.P. Mackenzie, S.R. Julian, A. Carrington, J.W. Loram, and J.R. Cooper, Phys. Rev. B **51**, 9375 (1995).

[11] Y. Dalichaouch, B.W. Lee, C.L. Seaman, J.T. Markert, and M.B. Maple, Phys. Rev. Lett. **64**, 599 (1990).

[12] A. Carrington, A.P. Mackenzie, and A. Tyler, Phys. Rev. B **54**, R3788 (1996).

[13] G. Blumberg, Moonsoo Kang, and M.V. Klein, Phys. Rev. Lett. **78**, 2461 (1997).

[14] C. Bergemann, A.W. Tyler, A.P. Mackenzie, J.R. Cooper, S.R. Julian, and D.E. Farrell, Phys. Rev. B **57**, 14 387 (1998).

[15] G.S. Boebinger, Y. Ando, A. Passner, T. Kimura, M. Okuya, J. Shimoyama, K. Kishio, K. Tamasaku, N. Ichikawa, and S. Uchida, Phys. Rev. Lett. **77**, 5417 (1996).

[16] Y. Ando, G.S. Boebinger, A. Passner, N.L. Wang, C. Geibel, and F. Steglich, Phys. Rev. Lett. **77**, 2065 (1996); **79**, 2595(E) (1997).

[17] Y. Ando, G.S. Boebinger, A. Passner, T. Kimura, and K. Kishio, Phys. Rev. Lett. **75**, 4662 (1995).

[18] Q. Li, M. Suenaga, T. Kimura, and K. Kishio, Phys. Rev. B **47**, 11 384 (1993).

[19] U. Welp, W.K. Kwok, G.W. Crabtree, K.G. Vandervoort, and J.Z. Liu, Phys. Rev. Lett. **62**, 1908 (1989).

[20] H. Safar, P.L. Gammel, D.A. Huse, D.J. Bishop, J.P. Rice, and D.M. Ginsberg, Phys. Rev. Lett. **69**, 824 (1992).

[21] J.L. Tallon, G.V.M. Williams, C. Bernhard, D.M. Pooke, M.P. Staines, J.D. Johnson, and R.H. Meinhold, Phys. Rev. B **53**, R11 972 (1996).

[22] A.S. Alexandrov, Phys. Rev. B **48**, 10 571 (1993); A.S. Alexandrov, V.N. Zavaritsky, W.Y. Liang, and P.L. Nevsky, Phys. Rev. Lett. **76**, 983 (1996).

[23] Y. Ovchinnikov and V. Kresin, Phys. Rev. B **52**, 3075 (1995).

[24] G. Kotliar and C.M. Varma, Phys. Rev. Lett. **77**, 2296 (1996).

[25] T. Koyama and M. Tachiki, Physica C **263**, 25 (1996).